euronoise

Optimization of compact finite difference method for wave acoustic simulation

Hideo Tsuru[a] and Reima Iwatsu[b]

[a]Nittobo Acoustic Engineering, 1-21-10 Midori Sumida-ku, 130-0021 Tokyo, Japan
[b]Tokyo Denki University, Kanda-Nishikicho 2-2, Chiyoda-ku, 101-8457 Tokyo, Japan
tsuru@noe.co.jp

Recently, a wave acoustic simulation becomes a useful tool for considering a method for noise reductions. The finite difference method in time domain is often used in wave acoustic simulations. The accuracy of this method depends on numerical dissipation and dispersion caused by finite difference approximation and time integration. A compact finite difference can reduce numerical dispersion of space derivative. Therefore, an optimization method of the compact finite difference is investigated. In order to improve time integration, a symplectic integration technique is adopted and excellent long time behavior is obtained.

1 Introduction

Recent development of computer technology enables us to carry out wave acoustic simulation for considering noise reduction. A wave nature of sound plays an important role in the prediction of noise. A finite difference method is easy to construct a numerical model from a physical model compared to the boundary element method or finite element method. The finite difference method often simulates wave propagations in time domain (FDTD) and enables us to grasp transient phenomena of sound.

In order to make an accurate simulation, a numerical dispersion which artificially makes propagation velocity different according to wave length, must be eliminated. A compact finite difference method effectively suppresses the numerical dispersion. We have optimized the coefficients in the compact finite difference.

First, the basic equation of sound propagation is described. Next, an optimization scheme of compact finite difference shall be discussed. Improvement techniques of time integrations are also investigated. A one-dimensional benchmark problem is solved by the proposed method. The influence of numerical dispersion on the wave propagation is shown in the next section. The last section is devoted to the conclusion.

2 Basic equation of sound wave propagation

In order to consider the time evolution equation for sound propagation, the sound pressure p and the velocity vector $\boldsymbol{v}$ are coupled. Neglecting the attenuation and nonlinear effects, we obtain the coupled partial differential equations

$$\rho_0 \frac{\partial \boldsymbol{v}}{\partial t} = -\nabla p, \tag{1}$$

$$\frac{\partial p}{\partial t} = -\rho_0 c^2 \mathrm{div}\ \boldsymbol{v} + \rho_0 c^2 Q, \tag{2}$$

where Q is volume velocity, ρ_0 mean density and c, sound velocity, respectively. Though these equations seem simple, this fact does not mean that it is easy to carry out numerical simulations. As the attenuation term is absent, small errors can survive or diverge in numerical solutions.

In order to make the numerical model of the coupled partial differential equations, the variables are usually defined on a staggered grid. A staggered grid in 2-dimensional space is illustrated in Fig.1. The pressure is defined on the center of mesh and velocities, on the edges.

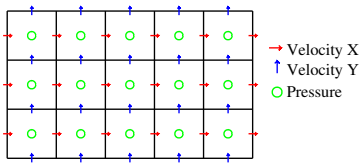

Figure 1: Staggered Grid

3 Optimized compact finite difference scheme

When accurate values of differentiations are required in a finite difference method, a grid spacing should be small compared to the typical wave length in the problem. Thus, for a high frequency problem, the grid spacing have to be small and the degree of freedom amounts to a huge value. In order to resolve this problem, a higher order or a compact finite difference can be applied [1]. The basic idea of the compact finite difference scheme is to couple differentiated values. Furthermore, the numerical dispersion of a compact finite difference on a uniform staggered grid can be minimized by adjusting coefficients. Introducing a parameter α, we consider a compact difference for a grid spacing h,

$$\begin{aligned} &\alpha f'_{i+1} + f'_i + \alpha f'_{i-1} \\ &= b\frac{f_{i+3/2} - f_{i-3/2}}{3h} + a\frac{f_{i+1/2} - f_{i-1/2}}{h} + e. \end{aligned} \tag{3}$$

Here, the coefficients a and b and the error term e are related by

$$a = \frac{3}{8}(3 - 2\alpha), b = \frac{22\alpha - 1}{8}, e = \frac{9 - 62\alpha}{1920} h^4 f^{(5)} \tag{4}$$

When $\alpha = 1/22$, the coefficient b vanishes and the compact finite difference is represented by a least number of grid points. Thus, this case is effective for the calculation around a complex obstacle. When $\alpha = 9/62$, the fourth order error term e vanishes and the difference equation becomes sixth order. We shall evaluate effective wave number k'. Effective wave number k' is defined by the function $f(x) = \sin(kx)$ and its first order differentiation $k' \cos(kx)$ evaluated by a finite difference. The normalized wave number $w = hk$ and normalized effective wave number $w' = hk'$ are defined by the grid spacing h. For example, $w = \pi/2$ means 4 grid points exist per one wave length (4ppw: point per wavelength). In the case of the second-order explicit finite difference on the staggered grid, w' becomes

$$w' = 2\sin(\frac{w}{2}). \tag{5}$$

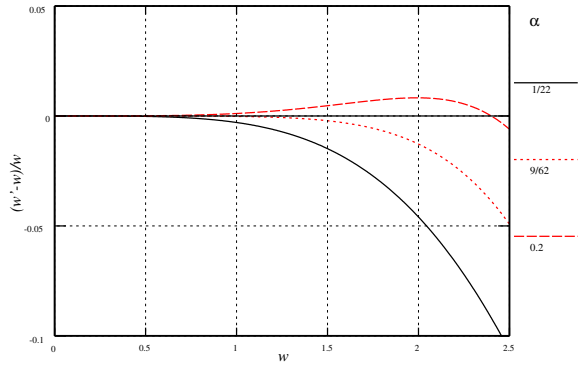

Figure 2: Relative error of effective wave number

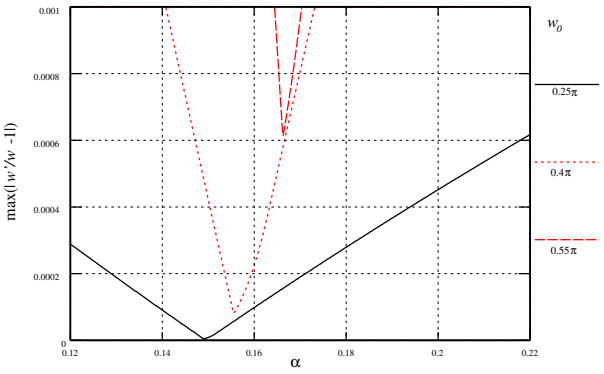

Figure 3: Maximum relative error

This deviates from the exact value when the normalized wave number is not very small. On the other hand, for the compact finite difference with parameter α, we obtain

$$w'(w,\alpha) = \frac{2a\sin(\frac{w}{2}) + \frac{2}{3}b\sin(\frac{3w}{2})}{1+2\alpha\cos(w)}. \tag{6}$$

The exact value is $w = w'$ and the difference from the exact value is numerical dispersion error. Some properties of w'

$$w'(0,\alpha) = 0, w'(\pi,\alpha) = \frac{7-10\alpha}{3(1-2\alpha)}, \tag{7}$$

$$w'(\pi,\alpha) < \pi, \text{ when } \alpha < \frac{3\pi-7}{6\pi-10} \approx 0.27 \tag{8}$$

can be derived. Therefore, when α is less than 0.27 and there is a point on which satisfies $w' > w$ in an interval $(0,\pi)$, then there exits a point w_1 where $w = w'$, i.e.,

$$w'(w_1,\alpha) = w_1. \tag{9}$$

Considering the sign of the error term near the origin, when $\alpha > 9/62$, the curve $w'(w,\alpha)$ is larger than the line of exact wave number around origin. When the α is small, the effective wave number becomes less than the theoretical value even if the ppw is not so small. On the other hand, when α is large, the effective wave number can approximate well the theoretical value up to the region of short wave length. In that case, the point w_1 and parameter α are related by

$$\alpha = \frac{27\sin(\frac{1}{2}w_1) - \sin(\frac{3}{2}w_1) - 12w_1}{18\sin(\frac{1}{2}w_1) - 22\sin(\frac{3}{2}w_1) + 24w_1\cos(w_1)}. \tag{10}$$

Therefore, adjusting the parameter of α can improve the finite difference according to the target frequency of the numerical analysis. The relative error $(w'-w)/w$ is shown in Fig.2. In order to optimize α, we have adopted the following strategy. First, we shall set the maximum frequency to be analyzed and corresponding normalized wave number w_0 are calculated. Next, the parameter α is determined so that the maximum value of a relative error in the interval of $(0, w_0)$ is minimized.

Table 1: Maximum wave number w_0, optimized α and maximum relative error

w_0	point per wave length (ppw)	optimized α	relative error
0.25π	8	0.14905	4.5×10^{-6}
0.3π	6.67	0.1508	1.4×10^{-5}
0.35π	5.71	0.15295	3.5×10^{-5}
0.4π	5	0.15555	8.1×10^{-5}
0.45π	4.44	0.15855	1.7×10^{-4}
0.5π	4	0.1621	3.3×10^{-4}
0.55π	3.64	0.16625	6.1×10^{-4}
0.6π	3.33	0.17100	1.1×10^{-3}

The maximum relative error up to maximum normalized wave number w_0 is plotted in Fig.3 where horizontal axis means α. The minimization of the maximum relative error can be attained through adjusting the parameter α. In Table 1, maximum wave number, optimized α and maximum relative error are shown. Thus, we can carry out accurate simulation through a relative large grid spacing.

4 Improvement of time integration

As the time integration is carried out in FDTD, our next aim is to improve the time marching operation. Here, we consider two types of integration techniques, the first one is linear multistep method and the second one, a symplectic integration [2, 3]. At first, let us examine the linear multistep method. Hereafter, the exact time derivative of function f is represented by F. The most simple time integration formula is

$$\frac{f(t+\Delta t) - f(t)}{\Delta t} = F(t + \frac{\Delta t}{2}). \tag{11}$$

In order to improve accuracy of the time evolution, a method in which multiple time step values of $F(t)$ are utilized to carry out the time integration, can be considered. We consider a numerical integration

$$\frac{f(t+\Delta t) - f(t)}{\Delta t} = b_0 F(t + \frac{\Delta t}{2}) + b_1 F(t - \frac{\Delta t}{2})$$

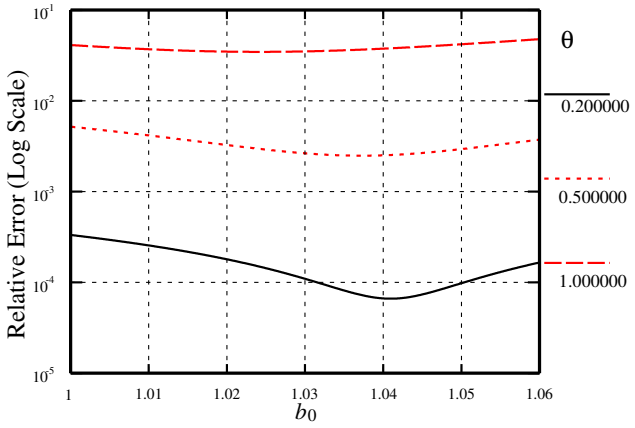

Figure 4: Relative error to b_0

$$+b_2 F(t - \frac{3\Delta t}{2}). \quad (12)$$

In this case, the coefficients $b's$ are related by

$$b_1 = (2 - 2b_0), \quad b_2 = (b_0 - 1). \quad (13)$$

When $b_0 = 1$, the eq. (12) reduced to one step integration which is usually used in FDTD. An improvement of the integration can be made by adjusting the parameter b_0. We shall consider a test function $f(t) = \exp(i\omega t)$, with angular frequency ω and also suppose that the time differentiations of the test function at the time $t + \Delta t/2, t - \Delta t/2, t - 3\Delta t/2$ are exactly obtained. By angular frequency ω and time step Δt, the normalized angular frequency $\theta = \omega \Delta t$ is defined. The parameter b_0 is optimized in order that the absolute value of difference between the exact value of f on the step $t+\Delta t$

$$f(t + \Delta t) = f(t) \exp(i\theta) \quad (14)$$

and the numerical value

$$\tilde{f}(t + \Delta t) = f(t)[1 + i\theta(b_0 \exp(i\frac{\theta}{2}) + b_1 \exp(-i\frac{\theta}{2}) + b_2 \exp(-i\frac{3\theta}{2}))] \quad (15)$$

is minimized. The parameter b_0 as function of θ in order to minimize the relative error err

$$err = |\frac{\tilde{f}(t + \Delta t) - f(t + \Delta t)}{f(t + \Delta t)}|. \quad (16)$$

The relative error is plotted in Fig.4. Each line represent θ and the minimum value versus b_0 is obtained. For various θ's, the optimum parameter are shown in Table 2. As a comparison, the error for the case of $b_0 = 1$ which corresponds to the one step integration is also shown. When the normalized angular frequency is small, the effect of the improvement is large. In FDTD calculations, this multistep integration is applied to both sound pressure and velocity vector evolutions. As the amount of finite difference calculations per one time step marching by this method is the same as the normal one, the improvement can be fulfilled without much augmentation of calculation time. On the other hand, the finite difference calculation must be carried out in each intermediate time step in the higher order Runge-Kutta method and the amount of calculation is multiplied.

Table 2: Normalized angular frequency, optimum b_0 and reletive error

Normalized θ	optimum b_0	Relative error	error for $b_0 = 1$
0.1	1.0415	4.16×10^{-6}	4.17×10^{-5}
0.5	1.037	2.49×10^{-3}	5.19×10^{-3}
1.0	1.024	3.46×10^{-2}	4.11×10^{-2}
1.5	1.0035	1.36×10^{-1}	1.36×10^{-1}

Table 3: Coefficient for Ruth's formula.

	1	2	3
b_i	7/24	3/4	-1/24
$\tilde{b}_i$	2/3	-2/3	1

Although multistep time integration can improve an accuracy in time marching, the effect is not large for a comparatively large time step. A symplectic integration which preserves several conservation quantities is a excellent scheme when the dynamics of the system is described by two or more variables and possesses a Hamiltonian structure. The symplectic integration scheme is developed for the last few decades and can be applied to particle dynamics, celestial mechanics and wave propagations [2, 3]. Although the theory of the symplectic integration is mainly developed in ordinary differential equation, extensions to a partial differential equation have been investigated recently [4, 5]. Here, we shall not go deep far into the symplectic integration for partial differential equation and apply Ruth's method to the differential equations for the acoustic propagation. In spite of its simplicity, the time integration can be done for long time with excellent accuracy.

We shall describe the out line of symplectic integral method. When a set of ordinary differential equations for variables p and q is described by the following form

$$\frac{dp}{dt} = f(q), \quad \frac{dq}{dt} = g(p) \quad (17)$$

The time marching by time step τ is carried out through m intermediate steps i,

$$P_i = P_{i-1} + \tau b_i f(Q_{i-1}) \quad Q_i = Q_{i-1} + \tau \tilde{b}_i g(P_i), \quad (18)$$

where

$$P_0 = p(t), Q_0 = q(t), P_m = p(t + \tau), Q_m = q(t + \tau) \quad (19)$$

The coefficients $b_i, \tilde{b}_i$ for Ruth's formula are shown in Table 3. For wave propagation, p and q considered acoustic pressure and velocity vector $\boldsymbol{v}$, respectively. Also $f(q)$ and $g(p)$ are described by the compact finite

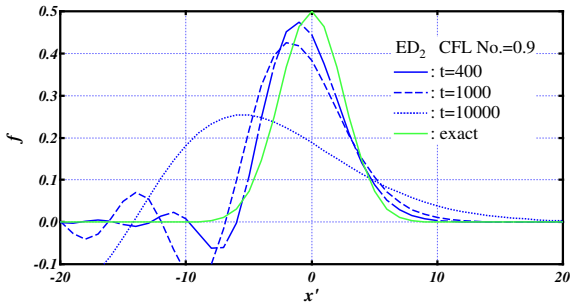

Figure 5: Wave form by primitive FDTD with CFL number=0.9.

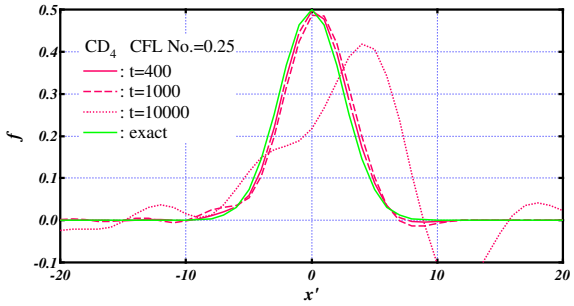

Figure 6: Wave form by fourth order compact finite difference and leap frog time integration with CFL number = 0.25.

differences of velocity vector $\boldsymbol{v}$ and pressure p, respectively.

The benchmark problem of 1-dimensional wave propagation has been carried out. We have set the initial wave form $f(x)$

$$f(x) = \frac{1}{2}\exp[-\ln 2(\frac{x}{3})^2], \tag{20}$$

and the grid spacing, $h = 1.0$ and the sound velocity 1.0. The simulations of wave propagation are done up to 10000 time step. The resulting shapes are illustrated in Figs.5-7. In each Figure, the center of mass is shifted.

The result obtained by optimized fourth order finite difference with parameter $\alpha = 0.1475$ and Ruth's time integration scheme is excellent. Even at the time step 10000, the wave shape almost retains the orignal form

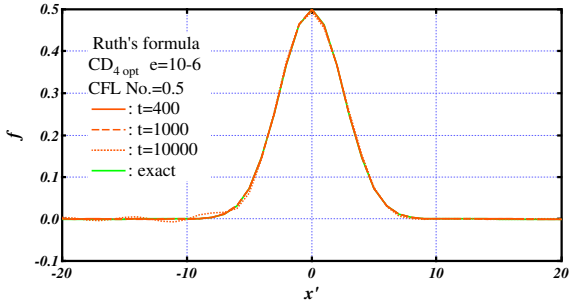

Figure 7: Wave form by optimized fourth order compact finite difference ($\alpha = 0.1475$) and Ruth's time integration with CFL number= 0.5.

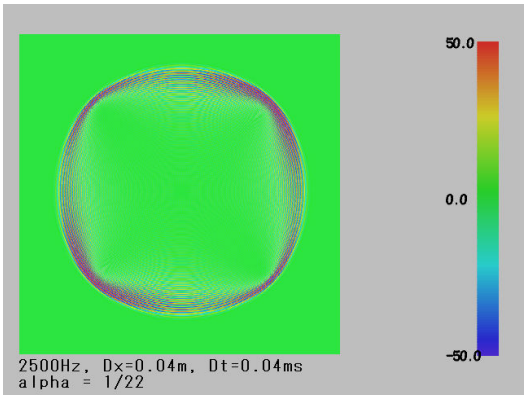

Figure 8: Instantaneous sound pressure for $\alpha = 1/22$

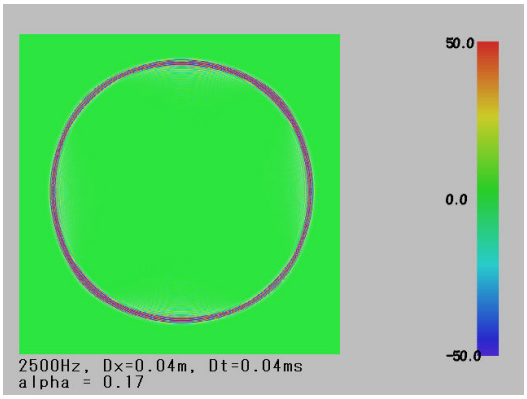

Figure 9: Instantaneous sound pressure for $\alpha = 0.17$

by this scheme. Therefore, for a long time step computation, the symplectic integration is highly effective.

5 Visualization and auralization of numerical dispersion

The influence of the numerical dispersion on the simulation can be recognized through visualization and auralization. As a large portion of numerical dispersion is caused by the truncation errors in the finite difference operations, the numerical dispersions by spatial finite differences are investigated.

In order to visualize the numerical dispersion in multi dimensional space, 2-dimensional wave propagation is simulated. A point source is set Gaussian wave packet of central frequency 2500Hz in a free space. In simulations, the sound velocity, the grid spacing and the time step are set 340m/s, 40mm and 40μs, respectively. For various α's, instantaneous sound pressure distributions are illustrated in Figs.8,9. The error is remarkable when α is 1/22. On the other hand, for the case of $\alpha = 0.17$, the error is well suppressed and the obtained distribution has an almost concentric circle pattern.

Next, in order to investigate quality of the sound obtained by a numerical simulation through the optimized compact finite difference, we attempt the auralization by convolution. The wave number k on the grid spacing

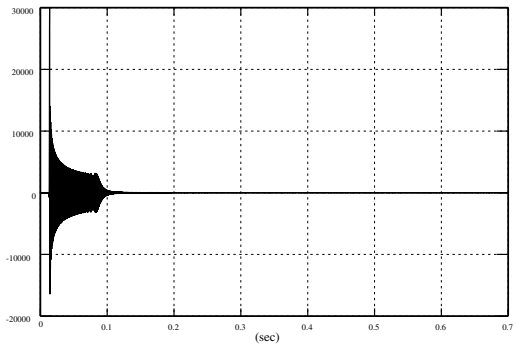

Figure 10: Response function by compact finite difference with $\alpha = 1/22$

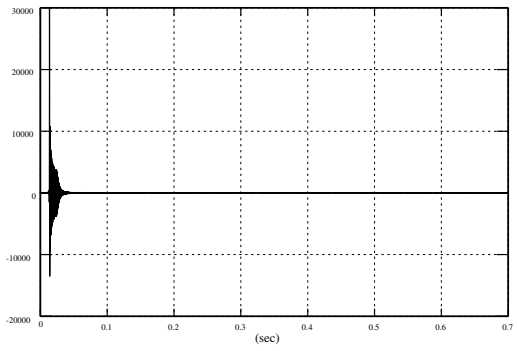

Figure 11: Response function by compact finite difference with $\alpha = 9/62$

h is related to the angular frequency ω by

$$\omega = \frac{c}{h}\frac{2a\sin(\frac{hk}{2}) + \frac{2}{3}\sin(\frac{3hk}{2})}{1 + 2\alpha\cos(hk)}. \qquad (21)$$

By eq.(21) we can evaluate the numerical phase velocity $c_p = \omega/k$. Then, the numerically delay time at the point at the distance of r from the source becomes $\Delta_\omega t = r/c_p$. The response function is calculated by adding each frequency component with a phase delay below the higher cut-off frequency. The auralization of a simulation result is fulfilled through a convolution with the response function.

As an example, we supposed that the grid spacing is 20mm, the cut off frequency, 4kHz and the distance, 300m. The response functions in time domain with various α's are plotted in Figs.10-12. For each case, the origin of time is shifted properly. The response function through compact finite difference with $\alpha = 1/22$ is not at all an impulse like shape. Even by a compact finite difference, the numerical dispersion modifies the impulse shape when α is small. The convolutions with numerical impulse responses can make auralizations of simulated sound. We could recognize the improvement of sound quality by the reduction of the numerical dispersion attained by the optimization of coefficients in the compact finite difference.

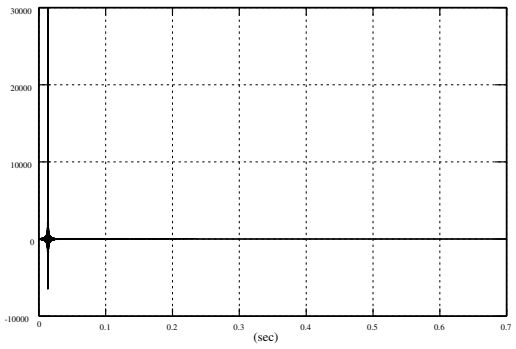

Figure 12: Response function by compact finite difference with $\alpha = 0.17$

By these examples, we can observe that the improvement of the scheme changes the simulated wave form qualitatively. Therefore, a highly accurate method is necessary for a prediction of sound propagation in practical situations.

6 Conclusion

We have shown the optimization of compact finite difference for the simulation of wave propagation. Through the optimization, the numerical dispersion is reduced up to higher frequency. A symplectic integration works well for time evolution of a wave and brings an excellent long time behavior. The influence of numerical dispersion have been also investigated and we have demonstrated that the highly accurate scheme is required for practical acoustic simulation.

References

[1] S. K. Lele, "Compact Finite-Difference Schemes With Spectral-Like Resolution." *J. Computational Physics. 103*, 16–42. (1992)

[2] R. D. Ruth, "A canonical integration technique", *IEEE Trans. Nuclear Sci. NS-30*, 2669-2671 (1983)

[3] H. Yoshida, "Construction of higher order symplectic integrators", *Physics Letters A 150*, 262–268. (1990)

[4] T.J.Bridges and S. Reich, "Multi-symplectic integrators: numerical schemes for Hamiltonian PDEs that conserve symplecticity", *Physics Letters A 284*. 184–193. (2001)

[5] J.E. Marsden, G. W. Patrick and S. Shkoller, "Multisymplectic Geometry, Variational Integrators and Nonlinear PDEs", *Comm. Math. Physics 199*, 351–395(1998)

[6] J. C. Hardin et al., ICASE/LaRC Workshop on Benchmark Problems in Computational Aeroacoustics (CAA), *NASA CP-3300*, (1995)